

Spin wave excitations in exchange-coupled [Co/Pd]-NiFe films with tunable tilting of the magnetization

S. Tacchi,¹ T. N. Anh Nguyen,² G. Carlotti,^{3,4} G. Gubbiotti,¹ M. Madami,³ R. K. Dumas,⁵ J. W. Lau,⁶ Johan Åkerman,^{2,5} A. Rettori,^{4,7} and M. G. Pini⁸

¹*Istituto Officina dei Materiali del CNR (CNR-IOM), Unità di Perugia, c/o Dipartimento di Fisica, Università di Perugia, I-06123 Perugia, Italy*

²*Materials Physics, School of Information and Communication Technology, KTH Royal Institute of Technology, Electrum 229, 16440 Kista, Sweden*

³*Dipartimento di Fisica, Università di Perugia, I-06123 Perugia, Italy*

⁴*Centro S3, c/o Istituto Nanoscienze del CNR (CNR-NANO), I-41125 Modena, Italy*

⁵*Department of Physics, University of Gothenburg, 41296 Gothenburg, Sweden*

⁶*National Institute of Standards and Technology, Gaithersburg, Maryland 20899, USA*

⁷*Dipartimento di Fisica, Università di Firenze, I-50019 Sesto Fiorentino (FI), Italy*

⁸*Istituto dei Sistemi Complessi del CNR (CNR-ISC), Unità di Firenze, I-50019 Sesto Fiorentino (FI), Italy*

(Received 15 March 2013; published 30 April 2013)

Brillouin light scattering was applied to measure the evolution of spin waves in exchange-coupled [Co/Pd]-NiFe films with out-of-plane/in-plane magnetic anisotropy. Tunable tilting of the magnetization has important effects on the spin wave frequency gap: a substantial increase is observed with decreasing the soft NiFe thickness, while seemingly insignificant tilting angles cause a strong reduction with respect to a film with only the hard [Co/Pd] component. The spin wave frequency is reproduced also in samples, with increased thickness of the upper Pd layer, where a sudden modification in the tilting at the hard/soft interface is caused by the weakening of interlayer exchange.

DOI: [10.1103/PhysRevB.87.144426](https://doi.org/10.1103/PhysRevB.87.144426)

PACS number(s): 75.70.Cn, 75.30.Ds, 75.60.Ej, 78.35.+c

The recent realization of nanodevices utilizing spin-transfer torque^{1–3} (STT) has demonstrated the tremendous potential it holds for novel spintronic devices and applications. Besides a renewed interest in understanding the transport properties of patterned magnetic heterostructures, these demonstrations have made clear the importance of also understanding the fundamental magnetodynamic eigenmodes in such structures; the switching speed of STT magnetoresistive random access memory, the maximum data rate and optimized noise properties of hard-drive read heads, and the operating frequency of spin-torque oscillators (STOs) all depend on the fundamental spin wave frequencies most easily excited under each respective operating condition. In uniformly magnetized nanocontact STOs with in-plane anisotropy,⁴ the two strongly nonlinear auto-oscillatory spin wave modes, the so-called propagating Slonczewski mode,^{5,6} and the localized Slavin-Tiberkevich soliton bullet,^{7,8} are either shifted slightly above^{5,7,9,10} or below^{6,8,10} the linear uniform ferromagnetic resonance (FMR) frequency of the free layer. In uniformly magnetized free layers with strong perpendicular magnetic anisotropy (PMA), the auto-oscillatory mode again lies slightly below the FMR frequency^{11–13} (except when a much more nonlinear and lower-frequency magnetic droplet soliton is nucleated¹⁴). The case when the uniformly magnetized free layer has a tilted anisotropy has also been investigated theoretically and experimentally.¹⁵ However, from both a theoretical and experimental viewpoint, the fundamental spin wave excitations in strongly nonuniform magnetic systems, such as exchange springs, offer both much richer magnetodynamic properties as well as much higher and more tunable STO frequencies in weak magnetic fields. While spin waves in in-plane magnetized exchange springs have been studied in detail,¹⁶

both theory and experiments are still missing for the recently demonstrated¹⁷ in-plane/out-of-plane exchange springs where the entire magnetization profile can be tuned with respect to both magnetization angle and degree of nonuniformity.

In the present work, Brillouin light scattering (BLS) has been exploited to study the dynamical magnetic properties of hard-soft [Co/Pd]-NiFe system as a function of both the soft film thickness t_{NiFe} and the intensity H of a magnetic field applied in the sample plane. The BLS data were analyzed using a theoretical model based on an accurate determination of the noncollinear canted ground-state configuration via a nonlinear map method,^{18–20} and the calculation of the magnetic excitation frequencies via the solution of linearized dynamic Landau-Lifshitz equations.²¹ We found that the magnetization orientation can be continuously tuned by changing t_{NiFe} or H . For small values of both parameters, one has the interesting case of composite hard-soft films with small tilting angles of the layer-by-layer magnetization from the perpendicular orientation, an arrangement very useful for STO applications^{22–24} such as zero-field operation; another unexpected and remarkable feature is that seemingly insignificant tilting angles (e.g., less than 1 degree in a composite film with $t_{\text{NiFe}} = 2.2$ nm and $H = 0.1$ kOe) cause a strong reduction of the spin wave frequency with respect to a film with only the hard [Co/Pd] component.

As described in Ref. 17, the samples were deposited on naturally oxidized Si(001) substrates by magnetron sputtering and have the following nominal layer structure: Ta(5 nm)/Pd(3 nm)/[Co(0.5 nm)/Pd(1 nm)]₅/NiFe(t_{NiFe}). The thickness of the hard phase [the [Co(0.5 nm)/Pd(1 nm)]₅ multilayer] was kept fixed^{17,25} to 7.5 nm, while the thickness of the soft one (the NiFe film) was varied between 2.2 and 7.5 nm, as calibrated from detailed transmission electron microscopy (TEM).²⁶ BLS

measurements were performed in backscattering geometry focusing about 200 mW of monochromatic light (532 nm wavelength) onto the sample surface. The backscattered light was analyzed by a Sandercock-type (3 + 3)-pass Fabry-Perot interferometer.²⁷ The external magnetic field H was applied parallel to the film surface and perpendicular to the plane of incidence of light. The incidence angle of light was 20°.

For data analysis, we use a one-dimensional model¹⁹ where the i th-layer magnetization M_i forms an angle θ_i with z , the normal to the film plane, and an angle ϕ_i with the in-plane x axis. N_h and N_s are the numbers of hard and soft layers, respectively. Letting $N = N_h + N_s$, the free-energy density is

$$E = - \sum_{i=1}^{N-1} \frac{A_{i,i+1}^{\text{ex}}}{d_{i,i+1}^2} [\sin \theta_i \sin \theta_{i+1} \cos(\phi_{i+1} - \phi_i) + \cos \theta_i \cos \theta_{i+1}] - \sum_{i=1}^N L_i \cos^2 \theta_i - \sum_{i=1}^N H^x M_i \sin \theta_i \cos \phi_i. \quad (1)$$

The quantity $L_i = K_i - 2\pi M_i^2$ is the effective anisotropy of the i th layer, with $L_i > 0$ corresponding to out-of-plane anisotropy; $A_{i,i+1}^{\text{ex}}/d_{i,i+1}^2$ denotes the exchange coupling between two neighboring layers, and $d_{i,i+1}$ denotes their distance; a magnetic field H is applied in plane along the x direction. The equilibrium configuration is provided by $\partial E/\partial \theta_i = 0$ and $\partial E/\partial \phi_i = 0$ ($i = 1, \dots, N$). The latter N equations are satisfied, $\forall i$, by $\phi_i = 0$; the former N equations can be reformulated, following Refs. 18–20, in terms of a two-dimensional nonlinear map

$$H_i^{\text{ex},+} s_{i+1} = H_i^{\text{ex},-} s_i + H_i^{\text{an}} \sin \theta_i \cos \theta_i - H^x \cos \theta_i, \quad (2)$$

$$\theta_{i+1} = \theta_i + \sin^{-1}(s_{i+1}),$$

where the auxiliary variables $s_i = \sin(\theta_i - \theta_{i-1})$ and the effective magnetic fields $H_i^{\text{ex},+} = A_{i,i+1}^{\text{ex}}/(d_{i,i+1}^2 M_i)$, $H_i^{\text{ex},-} = A_{i-1,i}^{\text{ex}}/(d_{i-1,i}^2 M_i)$, $H_i^{\text{an}} = 2L_i/M_i$ were introduced. With respect to continuum micromagnetic approaches,²⁸ the map preserves the discrete atomic structure of the film, thus it is applicable even in the case of strong changes in the layer-by-layer magnetization orientation (e.g., due to weakened interlayer exchange at the hard/soft interface). The equilibrium configurations are obtained within machine precision as the trajectories, in the (θ, s) phase space, which evolve in exactly N steps from $s_1 = \sin(\theta_1 - \theta_0) = 0$ to $s_{N+1} = \sin(\theta_{N+1} - \theta_N) = 0$.

The frequencies of spin wave excitations are obtained linearizing the Landau-Lifshitz equations of motion (γ is the gyromagnetic ratio):

$$\frac{d\theta_i}{dt} = - \frac{\gamma}{M_i \sin \theta_i} \frac{\partial F}{\partial \phi_i}, \quad \frac{d\phi_i}{dt} = \frac{\gamma}{M_i \sin \theta_i} \frac{\partial F}{\partial \theta_i}, \quad (3)$$

and diagonalizing a square matrix of rank $2N$ whose eigenvalues are real and can be ordered in pairs with equal norm and opposite sign.²¹ The smallest positive eigenvalue is the frequency of the uniform mode, experimentally accessible using BLS or FMR.

The magnetic parameters of the hard phase, $K_h = 6.3 \times 10^6$ erg/cm³ and $M_h = 365$ emu/cm³ were deduced from

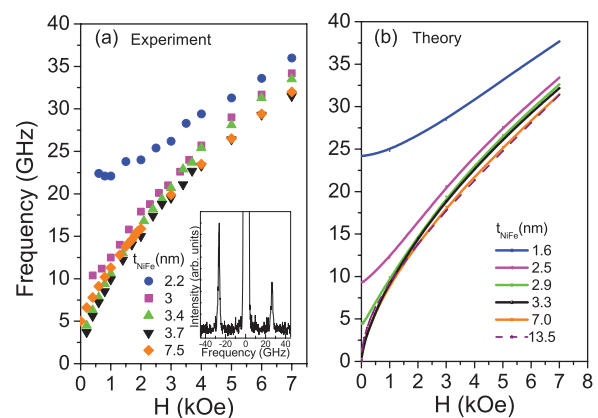


FIG. 1. (Color online) (a) Experimental and (b) calculated spin wave frequencies versus the intensity H of a magnetic field applied in plane for a composite [Co/Pd]₅-NiFe system with fixed thickness of the Co/Pd multilayer ($t_{\text{[Co/Pd]}} = 7.5$ nm) and variable thickness of the NiFe film (t_{NiFe}).

vibrating sample magnetometer measurements on a single [Co/Pd]₅ multilayer, while the hard-hard interlayer exchange $A_h^{\text{ex}} = 0.6 \times 10^{-6}$ erg/cm was obtained from a best fit of the out-of-plane remanence of the composite hard/soft material.¹⁷ For the NiFe layer we used the parameters $K_s = 0$ erg/cm³, $M_s = 687$ emu/cm³, and a soft-soft interlayer exchange $A_s^{\text{ex}} = 1.3 \times 10^{-6}$ erg/cm taken from the literature.²⁹ The hard-hard and soft-soft average interlayer distances, $d_h = 2.19 \times 10^{-8}$ cm and $d_s = 2.05 \times 10^{-8}$ cm, were deduced from structural measurements of the lattice parameters in Co/Pd multilayers³⁰ and NiFe films,³¹ respectively. In the absence of any direct experimental confirmation, at the hard/soft interface we assume^{16,20} $A_{hs}^{\text{ex}} = (A_h^{\text{ex}} + A_s^{\text{ex}})/2$ and $d_{hs} = (d_h + d_s)/2$.

Figure 1 shows a comparison between the measured (left panel) and the calculated (right panel) frequencies as a function of the intensity H of the applied magnetic field. To obtain a proper quantitative agreement between theory and experiment, the values of t_{NiFe} used in the calculation have been reduced by about 0.5 nm with respect to the values determined by TEM. This slight discrepancy can be attributed to the presence of a dead magnetic layer at the NiFe/Ta interface.³² It can be seen that for high NiFe thickness, the system exhibits a behavior similar to that of a magnetic film with easy-plane magnetization, characterized by a monotonic decrease of frequency versus field,²⁷ and a small (or vanishing) frequency gap as $H \rightarrow 0$. In contrast, as t_{NiFe} is reduced below a value of nearly 3 nm, a substantial frequency gap is clearly observed. The amplitude of this gap rapidly increases as the NiFe thickness is decreased in a the range of a few nanometers. Moreover, it should be noted that, at low field values ($H \leq 3$ kOe), the measured spin wave frequency of the composite hard/soft system presents a nonmonotonic dependence on t_{NiFe} . This trend is exemplified in Fig. 2, where the measured [Fig. 2(a)] and calculated [Fig. 2(b)] spin wave frequency is plotted against the NiFe film thickness for three values of the applied magnetic field. The nonmonotonic behavior of frequency on t_{NiFe} , calculated for $H \leq 1$ kOe, is in agreement with the experimental results.

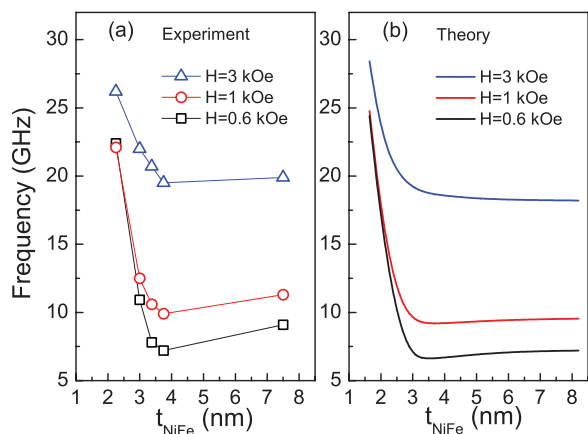


FIG. 2. (Color online) Dependence of (a) measured and (b) calculated spin wave frequency on thickness of soft phase, t_{NiFe} . The thickness of the hard phase is fixed to $t_{[\text{Co/Pd}]} = 7.5$ nm.

To achieve a deeper comprehension of the spin wave frequency behavior, it is very useful to consider the evolution of the magnetic ground state as a function of t_{NiFe} . Figure 3 shows the canting angle of the magnetization through the film thickness with respect to the film normal, calculated at different values of the magnetic field for three values of t_{NiFe} . For fixed H , the ground-state configuration strongly depends on the thickness of the soft layer, due to the competition between the in-plane and the out-of-plane anisotropy of the NiFe and [Co/Pd] layers, respectively. When the number of soft layers is large [Fig. 3(a)], the magnetization orientation varies over a wide range of angles through the film thickness: the magnetization gradually rotates from nearly perpendicular

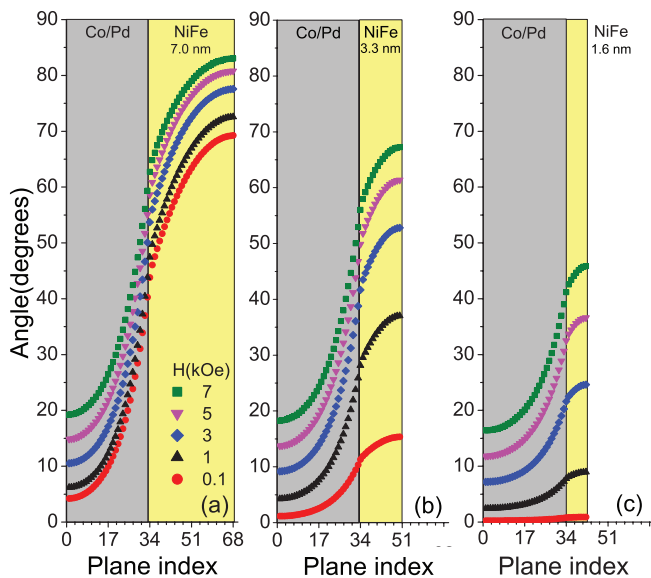


FIG. 3. (Color online) Canting angle with respect to film normal versus plane index ($i = 1, \dots, N = N_h + N_s$), calculated for a composite hard-soft system with a fixed thickness of hard phase ($t_{[\text{Co/Pd}]} = 7.5$ nm) and three NiFe thicknesses: (a) $t_{\text{NiFe}} = 7.0$ nm, (b) $t_{\text{NiFe}} = 3.3$ nm, (c) $t_{\text{NiFe}} = 1.6$ nm. Different symbols refer to selected values of H . The gray- and yellow-shadowed areas mark the Co/Pd multilayer and the NiFe film, respectively.

to the surface plane in the lowermost Co/Pd layers to nearly parallel to the surface plane in the topmost NiFe layers. Therefore, the frequency of spin wave excitations exhibits a rather small gap at zero field (Fig. 1). In the limiting case of a film with only the soft component (i.e., with a collinear parallel ground state), the spin wave frequency would vanish at zero field, because NiFe does not have any in-plane anisotropy. On the contrary, at low field one observes (Fig. 2) a slight increase in the spin wave frequency as t_{NiFe} is increased from 3.7 to 7.5 nm. This can be explained by considering that the canting angle of the hard layer increases with increasing number of soft layers, as seen in the calculated profiles of Figs. 3. This appreciable rotation of the magnetization of the hard phase with respect to the normal causes a correspondent increase in the anisotropy energy cost.

When the number of soft layers is reduced [Figs. 3(b) and 3(c)], the out-of-plane anisotropy of the hard phase becomes more pronounced, and the Co/Pd layer is able to rotate the magnetization in the NiFe film towards the direction perpendicular to the surface plane. This implies a high anisotropy-energy cost and an overall increase of the spin wave frequency. In particular, for an experimental NiFe thickness of 2.2 nm at $H = 0.1$ kOe [Fig. 3(c)] the Co/Pd underlayer is able to coherently rotate the whole NiFe layer; in fact, the canting angles of the NiFe layer are less than 1 degree. Such seemingly insignificant canting angles in the composite film are large enough to cause a strong reduction of the zero-field gap, $\nu = 24.2$ GHz, with respect to a film with only the hard [Co/Pd] component, where the theory predicts $\nu = \frac{\gamma}{2\pi} H_1^{\text{an}} = 89.8$ GHz.

As for the field dependence of the ground-state configuration, we note that, for all the investigated values of the applied field, a nonuniform angle configuration through the film thickness is found (see Fig. 3). As a consequence, the spin wave frequency does not present a minimum at a critical value of the magnetic field as usually observed³³ in magnetically hard films with a uniform perpendicular orientation of the layer-by-layer magnetization.

As a final remark, let us note that the above behavior is strongly dependent on the strength of the exchange coupling at the hard/soft interface. To quantitatively address this topic, we have also analyzed two more samples, both with $t_{\text{NiFe}} = 3.7$ nm, but where the thickness t_{Pd} of the final Pd layer at the interface was increased from 1 nm to 2 and 5 nm, respectively, as shown in Figs. 4(b) and 4(c), respectively.³⁴ This increase causes a strong suppression of the exchange coupling between the hard and the soft films, $A_{\text{hs}}^{\text{ex}}$, and results in a different dependence of the spin wave frequency on the field intensity. This is illustrated in Fig. 4(a): when the thickness of the upper Pd layer is 2 nm, the spin wave frequency exhibits an overall increase which can be well reproduced by the theoretical calculation if one assumes a reduction of the exchange coupling to one tenth [i.e., $A_{\text{hs}}^{\text{ex}} = \frac{1}{10}[(A_{\text{h}}^{\text{ex}} + A_{\text{s}}^{\text{ex}})/2]$]. The upward frequency shift is more apparent at high field, i.e., when the exchange coupling is weakened, and the magnetization of the Co/Pd multilayer is less canted with respect to the film normal [Fig. 4(b)] because the influence of the NiFe film, with easy-plane anisotropy, is reduced. In contrast, a further increase of the thickness of the upper Pd layer up to 5 nm causes a decrease of the spin wave frequency because, at such a

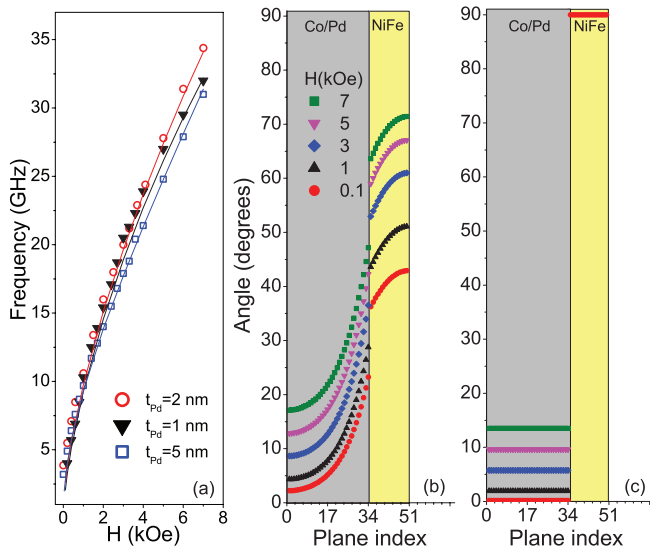


FIG. 4. (Color online) (a) Measured (symbols) and calculated (lines) spin wave frequency as a function of magnetic-field intensity H for composite $[\text{Co/Pd}]_5\text{-NiFe}$ films with fixed thickness of the NiFe film ($t_{\text{NiFe}} = 3.3$ nm) and variable thickness t_{Pd} of the final Pd layer at the interface. [(b) and (c)] Canting angle with respect to film normal versus layer index, calculated for composite hard-soft film with fixed thickness of hard ($t_{[\text{Co/Pd}]} = 7.5$ nm) and soft ($t_{\text{NiFe}} = 3.3$ nm) phase, for $A_{\text{hs}}^{\text{ex}} = (A_{\text{h}}^{\text{ex}} + A_{\text{s}}^{\text{ex}})/20$ and $A_{\text{hs}}^{\text{ex}} = 0$, respectively. The gray- and yellow-shadowed areas mark the Co/Pd multilayer and the NiFe film, respectively.

thickness, the hard and the soft phase are completely decoupled (i.e., $A_{\text{hs}}^{\text{ex}}$ vanishes), thus the NiFe layer behaves [Fig. 4(c)] as a standard in-plane-magnetized film.

In conclusion, we have applied the BLS technique to measure the evolution of spin waves in a composite hard/soft $[\text{Co/Pd}]\text{-NiFe}$ system. The delicate balance between the out-of-plane and the easy-plane anisotropy terms produces variations in the ground state and thus measurable differences in the spin wave excitation frequency. The theoretical approach was able to successfully account for the crossover between two regimes. For high NiFe thickness, the magnetization of the layers turn towards the film plane, and the spin wave frequency gap at zero field is rather small (a few GHz); for low NiFe thickness, the magnetization of the layers turns perpendicular to the film plane, and the spin wave frequency at zero field has a substantial gap (tens of GHz), proportional to the effective out-of-plane anisotropy. Moreover, the introduction of a relatively thick nonmagnetic Pd spacer results in a sudden transition of the magnetization configuration at the hard/soft interface, due to the weakening of the exchange coupling between the Co/Pd and the NiFe layer. Finally, we observe that measuring the energy of spin wave excitations definitely proves to be a more sensitive tool, with respect to static magnetometry, to investigate the highly nonuniform magnetic anisotropy in composite hard-soft films.

The research leading to these results has received partial financial support from MIUR under PRIN 2010-2011 “DyNanoMag”-prot. 2010ECA8P3. Support from the Swedish Foundation for strategic Research (SSF), the Swedish Research Council (VR), and the Swedish Institute (SI) is gratefully acknowledged. Johan Åkerman is a Royal Swedish Academy of Sciences Research Fellow supported by a grant from the Knut and Alice Wallenberg Foundation.

- ¹J. C. Slonczewski, *J. Magn. Magn. Mater.* **159**, 1 (1996).
- ²L. Berger, *Phys. Rev. B* **54**, 9353 (1996).
- ³D. Ralph and M. Stiles, *J. Magn. Magn. Mater.* **320**, 1190 (2008).
- ⁴T. J. Silva and W. H. Rippard, *J. Magn. Magn. Mater.* **320**, 1260 (2008).
- ⁵J. C. Slonczewski, *J. Magn. Magn. Mater.* **195**, 261 (1999).
- ⁶M. Tsoi, A. G. M. Jansen, J. Bass, W.-C. Chiang, M. Seck, V. Tsoi, and P. Wyder, *Phys. Rev. Lett.* **80**, 4281 (1998).
- ⁷A. Slavin and V. Tiberkevich, *Phys. Rev. Lett.* **95**, 237201 (2005).
- ⁸W. H. Rippard, M. R. Pufall, and T. J. Silva, *Appl. Phys. Lett.* **82**, 1260 (2003).
- ⁹M. Madami, S. Bonetti, G. Consolo, S. Tacchi, G. Carlotti, G. Gubbiotti, F. Mancoff, M. A. Yar, and J. Åkerman, *Nat. Nanotechnol.* **6**, 635 (2011).
- ¹⁰S. Bonetti, V. Tiberkevich, G. Consolo, G. Finocchio, P. Muduli, F. Mancoff, A. Slavin, and J. Åkerman, *Phys. Rev. Lett.* **105**, 217204 (2010).
- ¹¹W. H. Rippard, A. M. Deac, M. R. Pufall, J. M. Shaw, M. W. Keller, S. E. Russek, G. E. W. Bauer, and C. Serpico, *Phys. Rev. B* **81**, 014426 (2010).
- ¹²S. M. Mohseni, S. R. Sani, J. Persson, T. N. Anh Nguyen, S. Chung, Y. Pogoryelov, and J. Åkerman, *Phys. Status Solidi RRL* **5**, 432 (2011).
- ¹³S. M. Mohseni, S. R. Sani, J. Persson, T. N. Anh Nguyen, S. Chung, Ye. Pogoryelov, P. K. Muduli, E. Iacocca, A. Eklund, R. K. Dumas, S. Bonetti, A. Deac, M. A. Hofer, and J. Åkerman, *Science* **339**, 1295 (2013).
- ¹⁴M. A. Hofer, T. J. Silva, and M. W. Keller, *Phys. Rev. B* **82**, 054432 (2010).
- ¹⁵C. L. Zha, J. Persson, S. Bonetti, Y. Y. Fang, and J. Åkerman, *Appl. Phys. Lett.* **94**, 163108 (2009).
- ¹⁶E. E. Fullerton, J. S. Jiang, M. Grimsditch, C. H. Sowers, and S. D. Bader, *Phys. Rev. B* **58**, 12193 (1998).
- ¹⁷T. N. Anh Nguyen, Y. Fang, V. Fallahi, N. Benatmane, S. M. Mohseni, R. K. Dumas, and J. Åkerman, *Appl. Phys. Lett.* **98**, 172502 (2011).
- ¹⁸L. Trallori, P. Politi, A. Rettori, M. G. Pini, and J. Villain, *Phys. Rev. Lett.* **72**, 1925 (1994).
- ¹⁹L. Trallori, M. G. Pini, A. Rettori, M. Macciò, and P. Politi, *Int. J. Mod. Phys. B* **10**, 1935 (1996).
- ²⁰M. Amato, M. G. Pini, and A. Rettori, *Phys. Rev. B* **60**, 3414 (1999).
- ²¹M. Ramesh and P. E. Wigen, *J. Magn. Magn. Mater.* **74**, 123 (1988).
- ²²S. Mangin, D. Ravelosona, J. A. Katine, M. J. Carey, B. D. Terris, and E. E. Fullerton, *Nat. Mater.* **5**, 210 (2006).

- ²³X. C. Zhu and J.-G. Zhu, *IEEE Trans. Magn.* **42**, 2739 (2006).
- ²⁴R. Sbiaa, R. Law, E.-L. Tan, and T. Liew, *J. Appl. Phys.* **105**, 013910 (2009).
- ²⁵R. Sbiaa, O. K. Aung, S. N. Piramanayagam, E. Tan, and R. Law, *J. Appl. Phys.* **105**, 073904 (2009).
- ²⁶Please note that the nominal thicknesses of the present set of samples are the same as those of Ref. 17. However, a refined transmission electron microscopy analysis permitted us to verify that the previously indicated values of NiFe thickness were overestimated by about 25 percent.
- ²⁷G. Carlotti and G. Gubbiotti, *Riv. Nuovo Cimento* **22**, 1 (1999).
- ²⁸G. Asti, M. Ghidini, R. Pellicelli, C. Pernechele, M. Solzi, F. Albertini, F. Casoli, S. Fabbri, and L. Pareti, *Phys. Rev. B* **73**, 094406 (2006).
- ²⁹C. J. Kinane, A. K. Suszka, C. H. Marrows, B. J. Hickey, D. A. Arena, J. Dvorak, T. R. Charlton, and S. Langridge, *Appl. Phys. Lett.* **89**, 092507 (2006).
- ³⁰S. K. Kim, J. S. Kang, J. I. Jeong, J. H. Hong, Y. M. Koo, H. J. Shin, and Y. P. Lee, *J. Appl. Phys.* **72**, 4986 (1992).
- ³¹J. Singh, S. K. Gupta, A. K. Singh, P. Kothari, R. K. Kotnala, and J. Akhtar, *J. Magn. Magn. Mater.* **324**, 999 (2012).
- ³²Q. Leng, H. Han, M. Mao, C. Hiner, and F. Ryan, *J. Appl. Phys.* **87**, 6621 (2000).
- ³³J. R. Dutcher, J. F. Cochran, I. Jacob, and W. F. Egelhoff, *Phys. Rev. B* **39**, 10430 (1989).
- ³⁴T. N. Anh Nguyen, N. Benatmane, V. Fallahi, Y. Fang, S. M. Mohseni, R. K. Dumas, and J. Åkerman, *J. Magn. Magn. Mater.* **324**, 3929 (2012).